

Article

An Optically Augmented Visual Aid for Individuals with Age-Related Macular Degeneration

Nahed H. Solouma ^{1,*}, Noura Negm ², Hafsah Ahmad ¹ and Yusuf Gamal ^{2,*}

¹ College of Engineering, King Faisal University, P.O. Box 400, Al-Ahsa 31982, Saudi Arabia; hahmad@kfu.edu.sa

² Department of Engineering Applications of Lasers, National Institute of Laser Enhanced Sciences, Cairo University, Giza 12613, Egypt; negm_nora@yahoo.com

* Correspondence: nsolouma@kfu.edu.sa (N.H.S.); yusuf.gamal@cu.edu.eg (Y.G.)

Abstract: Normal vision is a precious gift to mankind. Any vision defect or degradation is actually an intimidating problem for individuals and societies. Therefore, researchers are continually working to find effective solutions for vision disorders. In some retinal diseases such as Age-related Macular Degeneration (AMD), visual aids are required to improve vision ability and/or stop the progress of the disease. Recently, augmented vision techniques have been used to provide aid to people suffering from retinal impairment. However, in such techniques, the images of real scenes are electronically deformed to compensate for vision impairment. Therefore, the natural scene is displayed as an electronic image on glasses. Intuitively, it is annoying to the patient to see electronic rather than natural scenes. Moreover, these visual aids are bulky and produce electric fields that might be harmful with continuous use. In this work, a novel optical solution to provide a visual aid to patients with central vision loss has been proposed. The proposed optical solution deforms the wavefront of the scene to entirely fall on the healthy parts of the retina. This, in turn, conveys all scene information to the brain to be perceived by the patient. As it provides optical processing, the proposed solution overcomes all drawbacks of the electronic solutions. To prove the validity of the proposed solution, three lenses were designed, fabricated, and tested to visualize simple shapes, reading, and obtaining aid during walking and driving. Obtaining the expected results from these tests, they were tried by three volunteers to clinically prove the validity and feasibility of the proposed optical aid. The feedback from the three patients was promising since all of them could recognize some of the details they used to miss with at least one of the lenses.



Citation: Solouma, N.H.; Negm, N.; Ahmad, H.; Gamal, Y. An Optically Augmented Visual Aid for Individuals with Age-Related Macular Degeneration. *Photonics* **2024**, *11*, 245. <https://doi.org/10.3390/photonics11030245>

Received: 17 January 2024
Revised: 25 February 2024
Accepted: 6 March 2024
Published: 8 March 2024



Copyright: © 2024 by the authors. Licensee MDPI, Basel, Switzerland. This article is an open access article distributed under the terms and conditions of the Creative Commons Attribution (CC BY) license (<https://creativecommons.org/licenses/by/4.0/>).

Keywords: retinal disorders; retinal impairment; AMD; augmented reality; visual aids; Bi-cone lens; optical visual aids

1. Introduction

According to the World Health Organization (WHO), about 285 million people (4.25% of the world's population) have visual impairment. Almost thirty-nine million of them are totally blind and about 246 million have low vision performance. Nearly 256 million people suffering from vision impairments live in developing countries, among these countries is Egypt, of which three million of its population suffer from vision impairment and more than one million of them are blind [1,2]. Such a pathetic figure motivates the researchers to find solutions to keep and hopefully restore vision and provide visual aids [3].

There are many vision disorders that may cause sight degradation and/or vision loss, including cataracts, glaucoma, refractive errors, corneal and lens opacities, and retinal diseases [4,5]. The disorders related to the optical parts of the eye can be treated optically and/or surgically [6,7]. Unfortunately, retinal diseases have no curative treatment but only trials to stop the progress of the diseases and prevent blindness [8–10]. Vision aids are usually proposed to patients with retinal disorders. The patients need to be trained and become accommodated with such aids to help them move safely.

Entering the eye, light from scenes or the wavefront is focused on the retina by the optical parts of the eye, namely the cornea and the lens, as shown in Figure 1. The retina is a membrane full of a specific type of neural cells called photoreceptors which can convert light into sequences of electric pulses. The sequences of pulse are transmitted to the brain, via the optic disc, to get processed and be perceived as an image. The optic disc itself is the bundle of nerves of the photoreceptors. The photoreceptors are divided into two types: rods and cones, as shown in Figure 1. Rods are very sensitive to light and hence they enable us to see at night. Cones enable us to visualize and distinguish colors and present in three types sensitive to red, green, and blue light [4,5]. As the retina is composed of neurons, damaged parts of the retina cannot be cured. Trials are always conducted to prevent the spread of such damage [8–10].

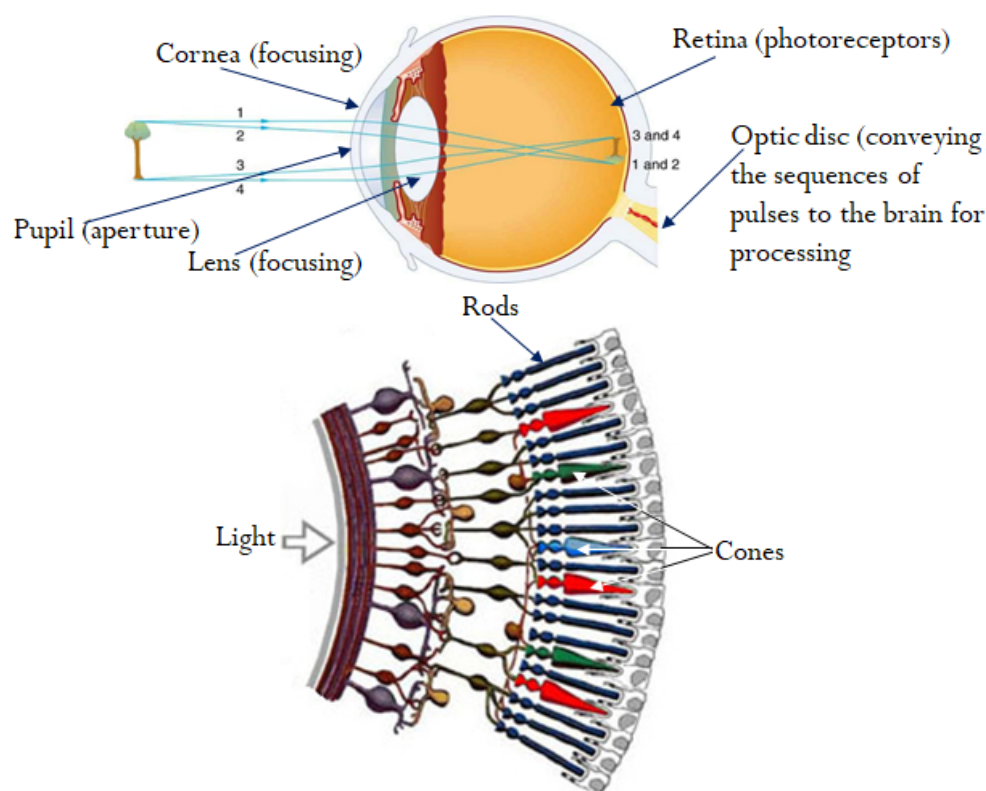


Figure 1. Simple eye anatomy. Upper: propagation of light rays number 1,2,3 and 4 show the wavefront until forming the image on the retina. Lower: a section of the retina showing different layers, the rods, and the cones [5].

The retina takes nutrition from the blood vessels in a layer behind it called the choroid [5]. As complications of some diseases, hemorrhage or leakage may occur and exudate is formed between the retina and the choroid in some parts. This leads to the detachment of these parts of the retina from the choroid. The photoreceptors of such parts get irreversibly damaged and lose their functions [10]. Light incidents on damaged parts cannot be converted into sequences of electric pulses. Consequently, the corresponding part of the scene is missed from the image perceived by the brain and the patient sees black parts instead [11,12].

The central part of the retina is called the macula which has the fovea inside it. The macula with the fovea enables our sharpest vision [13]. With age and some diseases, the macula may get damaged in a disorder called age-related macular degeneration AMD [13]. There are many other diseases that may affect the retina such as retinitis pigmentosa and vasculature disorders. Retinitis pigmentosa (RP) is a clinically and genetically heterogeneous group of inherited retinal diseases. It is a progressive retinal disorder that is

characterized by retinal pigment deposits when monitored with fundus photographs [13]. Vasculature diseases are mainly due to complications of diabetes and are characterized by the presence of abnormal vasculatures such as neovessels, microaneurysms, and hemorrhage [14–16]. AMD is one of the most common vision impairments that lead to blindness worldwide. There are two types of AMD; dry and wet. About 90% of AMD patients have dry AMD [17]. In dry AMD, the retinal pigmented epithelium degrades gradually, leading to dystrophy (yellow spots called “drusen” cover the macula and the region around it). Dry AMD is considered an early stage of AMD, during which patients do not totally lose their ability to read. On the other hand, wet AMD is an advanced grade of AMD during which new tiny blood vessels named “neovessels” arise in the choroid. The presence of such vessels results in blood and fluid leakage. Additionally, the photoreceptors of the affected area in the macula are irreversibly damaged and the vision starts to degrade [18]. However, the spread of the neovessel can be stopped by laser photocoagulation [19,20].

Recent studies provide the most up-to-date developments in pharmacologic, gene, and stem-cell therapies to improve vision for patients with AMD [21–23]. In the same context, augmented reality enables visually impaired people to see as many details of real scenes as possible [24]. This is usually achieved by capturing a digital image of the real world, electronically processing this image, and displaying it on the glasses used by the patient [25]. The processing may be to demarcate some image features, change magnification, and/or apply spatial transformation according to the case, which, of course, differs from one patient to another. Thus, the augmented virtual reality system encompasses a camera, a processing unit, and a see-through display which makes it bulky and of offensive shape. Moreover, the patients using such systems view digital images rather than real-world scenes which is annoying and requires training and accommodation [26].

More than two decades ago, Lawton proposed the use of digital filtering to enhance the visual information for patients with retinal dystrophy. Her technique was used to digitally enhance the reading abilities of AMD patients. The experiments showed increased abilities in reading by 2 to 4 times [27]. Following Lawton, Peli et al. in [28] used two image enhancement methods: adaptive thresholding and adaptive enhancement filters to enhance the perception of face images. The first augmented vision solution for visually impaired people was proposed by Peli et al. [29]. Simulating the case of tunnel vision (where the patient can see only a narrow field of vision). The full scene is processed such that the edges are emphasized and the whole scene is demagnified to the field of vision of the patient. The central part of the whole scene that can be viewed by the patient is extracted and imposed (without processing) on the processed demagnified scene. Thus, the patient can see the central part naturally while having the salient information (edges) of the whole scene on a see-through display. However, the patients need to be trained on what they see and how can they interpret it because scene processing results in so-called “inattentional blindness”.

Furthermore, a head-mounted display (HMD) for low-vision people [30] and AMD and RP patients has been developed [31,32]. The system consists of three main parts: a mounted head with a fixed capturing camera, a video processing unit, and a see-through display. Captured videos are sent to the processing unit which magnifies the original scene and extracts edges from the main original scene by edge detection kernel. The processed scene is then superimposed on the original scene from the center with the same scale by the see-through display. The augmented vision enhancement has been also implemented on Google goggles to provide impaired vision people with a suitable visual aid [33]. The developed goggles give retinal impairment patients new possibilities for developing an accepted HMD with an appealing shape and compact design with a reasonable cost.

Since the macula is the central part of the retina, AMD patients lose the ability to see through the central region; instead, they depend on their peripheral vision. Current visual solutions are mainly based on the electronic aids utilizing HMD, as reported in [33]. HMDs are very expensive, bulky, and not patient-friendly as they provide electronic displays rather than natural scenes, produce an electric field and interference that is harmful with continuous use, and need complicated prescriptions and electronic maintenance processes.

In this work, an optical solution is proposed for AMD patients. The proposed solution provides spatial deformation of the light or wavefront coming from the scene. This deformation is completed by deflecting the light rays to obtain a total incident on the peripheral healthy parts of the retina. This leads to the perception of the salient features of the scene to compensate for central vision loss. As an optical solution, it utilizes a waveguide, which is a lens or pair of lenses used as glasses. Intuitively, the proposed optical solution overcomes most of the drawbacks of the electronic solutions as it provides natural scenes, is less expensive, is not bulky but is just glasses, is easy to fabricate, does not produce electric fields, and does not need special maintenance. Although the electronic solution provides real-time processing, it is not compared to optical processing, which is performed at the speed of light propagation.

2. The Proposed Waveguide Design

The proposed optically augmented visual aid is just a lens or pair of lenses to be used as glasses. Therefore, the lens acts as a spatial transformer waveguide to deflect the wavefront so that falls totally onto the healthy parts rather than the impaired central part of the retina. For appropriate design, the distance from the eye lens to the retina, the area of the damaged part on the retina or macula, and the area of the healthy peripheral retina are to be considered. On average, the distance from the human lens to the macula is 19 mm, as shown in Figure 2. The average area of the retina is 1094 mm² and that of the macula is about 28.25 mm². When the part of the macula is degenerated, the strength of vision degrades as well. In Figure 2, N and N' are the nodal points, p and p' indicate the position of the principal planes, and C is the point around it the eye-ball can be rotated inside its socket, which lies at a distance of 13.5 mm from the front vertex of the eye [34].

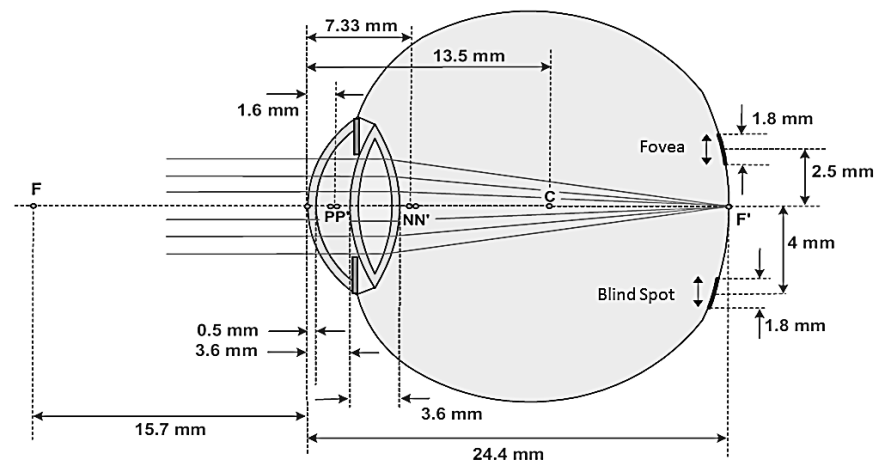


Figure 2. Geometrical structure of the eye and light focusing on the retina [34].

The proposed waveguide is a conical lens of three surfaces: two parallel coaxial conical surfaces and a cylindrical surface. The conical surfaces have the same height h and base-radius r . The thickness of the lens is d ; accordingly, the height of the cylindrical surface is $d \sin \varnothing$ where \varnothing is half of the cone apex angle. For patients with central vision loss, the apex of the conical lens is the proximal end of the goggle. Therefore, the real scene is spatially transformed to the periphery around the apex leaving a central blind circle as illustrated in Figure 3. From its structure, this proposed waveguide could be called a co-axial bi-cone lens or simply a bi-cone lens.

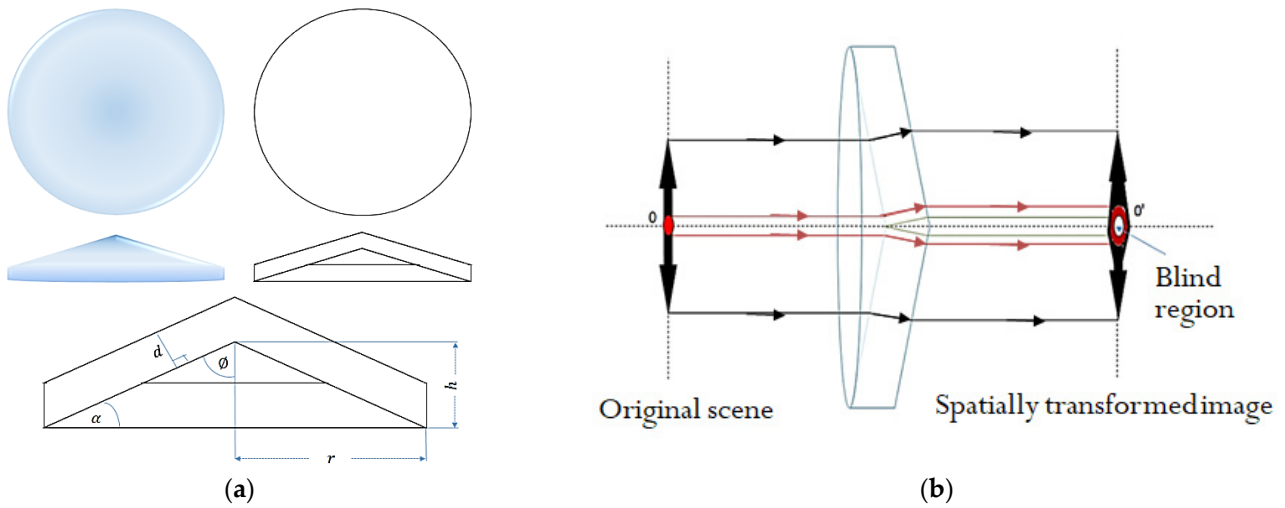


Figure 3. The proposed bi-cone lens. (a) Top, side, and front views of the lens and (b) schematic diagram of the bi-cone lens and its central spatial transformation effect illustrated by the red-colored rays.

2.1. Ray Tracing by Geometrical Optics for the Bi-Cone Lens

To analyze the bi-cone lens and illustrate the image formation, Snell’s law is applied to the upper half of the schematic diagram of the bi-cone lens, as shown in Figure 4. Ray tracing through the lower half is symmetric to ray tracing through the upper half.

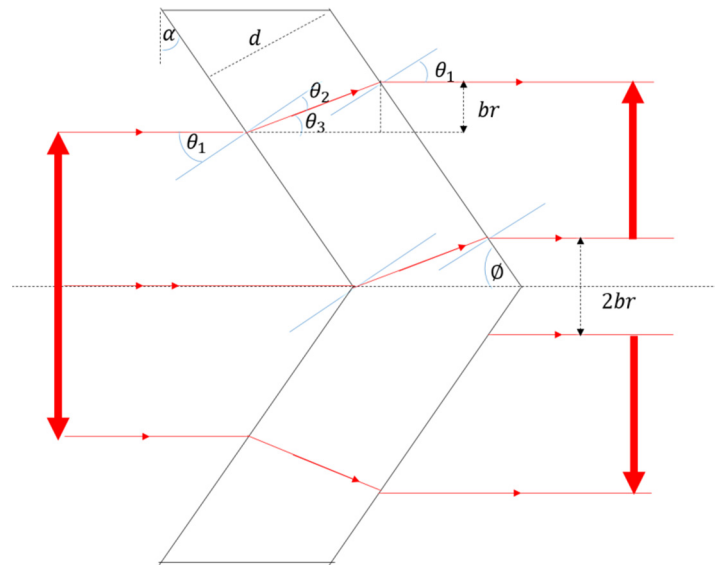


Figure 4. Geometrical ray tracing through the proposed bi-conical lens.

Figure 4 shows an incident ray parallel to the optical axis of the lens with θ_1 angles of incidence and θ_2 angle of refraction. Because the two surfaces (air–lens material and lens material–air) are parallel, the ray goes from lens to air with the same angle θ_1 as shown in Figure 4. To obtain a relation between the radius of the blind region br and the cone parameters, we use Snell’s law as follows:

$$\theta_2 = \sin^{-1} \left(\frac{n_1}{n_2} \sin \theta_1 \right) \tag{1}$$

where n_1 and n_2 are the refractive indices of air and lens material, respectively.

$$\cos \theta_2 = \frac{d}{x} \quad \text{and} \quad \sin \theta_3 = \frac{br}{x} \tag{2}$$

where x is the length of the ray inside the lens material and d is the thickness of lens. Therefore,

$$br = \frac{d}{\cos \theta_2} \sin \theta_3 \tag{3}$$

But $\theta_3 = \theta_1 - \theta_2$ and hence,

$$br = \frac{d \sin(\theta_1 - \theta_2)}{\cos \theta_2} \tag{4}$$

$$br = d \frac{\sin \theta_1 \cos \theta_2 - \cos \theta_1 \sin \theta_2}{\cos \theta_2} \tag{5}$$

$$br = d \left(\sin \theta_1 - \cos \theta_1 \tan \left(\sin^{-1} \left(\frac{\sin \theta_1}{n_2} \right) \right) \right) \tag{6}$$

For the rays parallel to the optical axis, $\theta_1 = \alpha = 90 - \varnothing$, which leads to:

$$br = d \left(\sin \alpha - \cos \alpha \tan \left(\sin^{-1} \left(\frac{\sin \alpha}{n_2} \right) \right) \right) \tag{7}$$

$$\therefore br = d \left(\cos \varnothing - \sin \varnothing \tan \left(\sin^{-1} \left(\frac{\cos \varnothing}{n_2} \right) \right) \right) \tag{8}$$

Therefore, the ray deviation distance or the radius of the blind region depends on the thickness of the lens, the cone apex angle, and the refractive index of the lens material. From Equations (7) and (8), the radius of the blind region br could be obtained by lens thickness d and either the base angle α or apex angle \varnothing . Figure 5a shows the blind region radius br against the cone base angle α for a material of refractive index $n = 1.49$ for two lens thicknesses, 1 mm and 2 mm. This relation indicates that br is directly proportional to d for specific α and n . Figure 5b shows the same relation for three waveguides of the same thickness, 2 mm, and different of refractive indices of 1.49, 1.52, and 1.6. This relation indicates a negligible dependency on the refractive index.

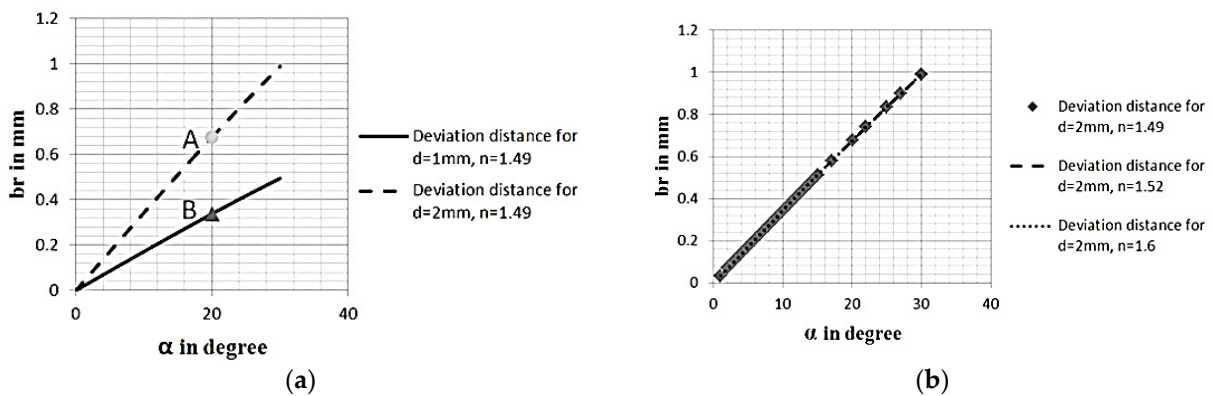


Figure 5. Relation between the deviation distance and the cone base angle. (a) Deviation distance or radius of blind region br against cone base angle α for two different bi-cone lenses and (b) deviation distance br against cone base angle α for three different lens materials.

2.2. Ray Tracing by Transfer Matrix for the Bi-Cone Lens

The ray transfer matrix gives the relationship between the output and input parameters of the ray crossing an optical system. These parameters specify the input and output points

where the ray enters and leaves the system. The point is specified by the distance of the point from a reference axis y and the angle the ray makes with this axis z . To analyze the bi-cone lens using the ray transfer matrix, the schematic diagram shown in Figure 6 is considered, in which the first and second surfaces are the air–lens and lens–air parallel surfaces. The input and output points are specified by $\begin{bmatrix} y_{in} \\ z_{in} \end{bmatrix}$ and $\begin{bmatrix} y_{out} \\ z_{out} \end{bmatrix}$, respectively.

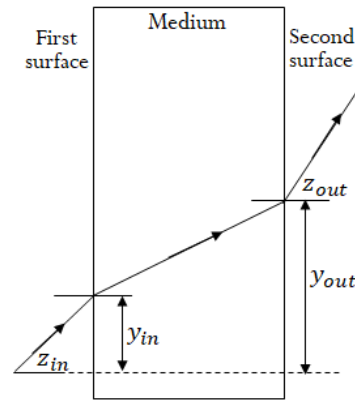


Figure 6. Ray tracing for ray matrix evaluation.

For this optical system, the ray transfer matrix is given by:

$$\begin{bmatrix} y_{out} \\ z_{out} \end{bmatrix} = \begin{bmatrix} A & B \\ C & D \end{bmatrix} \begin{bmatrix} y_{in} \\ z_{in} \end{bmatrix} \tag{9}$$

To obtain the ray transfer matrix $\begin{bmatrix} A & B \\ C & D \end{bmatrix}$ of the bi-cone lens, the ray is traced from the air to the lens material through the first surface, from the first to second surface through the lens material, and finally from the lens material to the air through the second surface. Through the first surface, the ray tracing is given by:

$$\begin{bmatrix} y_1 \\ z_1 \end{bmatrix} = \begin{bmatrix} 1 & 0 \\ 0 & \frac{n_1}{n_2} \end{bmatrix} \begin{bmatrix} y_{in} \\ z_{in} \end{bmatrix} \tag{10}$$

Through the lens material, the ray tracing is given by:

$$\begin{bmatrix} y_2 \\ z_2 \end{bmatrix} = \begin{bmatrix} 1 & \frac{d}{n_2} \\ 0 & 1 \end{bmatrix} \begin{bmatrix} y_1 \\ z_1 \end{bmatrix} \tag{11}$$

And through the second surface, the ray tracing is given by:

$$\begin{bmatrix} y_{out} \\ z_{out} \end{bmatrix} = \begin{bmatrix} 1 & 0 \\ 0 & \frac{n_2}{n_1} \end{bmatrix} \begin{bmatrix} y_2 \\ z_2 \end{bmatrix} \tag{12}$$

Substitute into Equation (9), the overall ray tracing is given by:

$$\begin{bmatrix} y_{out} \\ z_{out} \end{bmatrix} = \begin{bmatrix} 1 & 0 \\ 0 & \frac{n_2}{n_1} \end{bmatrix} \begin{bmatrix} 1 & \frac{d}{n_2} \\ 0 & 1 \end{bmatrix} \begin{bmatrix} 1 & 0 \\ 0 & \frac{n_1}{n_2} \end{bmatrix} \begin{bmatrix} y_{in} \\ z_{in} \end{bmatrix} \tag{13}$$

$$\begin{bmatrix} y_{out} \\ z_{out} \end{bmatrix} = \begin{bmatrix} 1 & \frac{d}{n_2} * \frac{n_1}{n_2} \\ 0 & 1 \end{bmatrix} \begin{bmatrix} y_{in} \\ z_{in} \end{bmatrix} \tag{14}$$

where the ray deviation distance br is given by:

$$br = y_{out} - y_{in}$$

2.3. The Experimental Investigations

Three experiments with three different handmade co-axial bi-cone ophthalmic lenses have been performed to investigate the spatial transformation of an image to the periphery. Two high-quality transparent materials with a refractive index of 1.49, commonly used for eyeglasses, were used to fabricate three lenses. These three lenses have different parameter values, as presented in Table 1. The values of the parameters were selected randomly with the technician for the ease of fabrication and proof of concept. These materials are Poly(allyl diglycol carbonate), technically known as CR-39 (Columbia Resin # 39), and Poly(methyl methacrylate), abbreviated as PMMA. The three experiments are described as follows:

Table 1. Lens’s parameters used for the three experiments.

	Experiment I	Experiment II	Experiment III
Lens material	CR-39	PMMA	CR-39
Refractive index n	1.49	1.49	1.49
Lens thickness d	1.5 mm	4 mm	1.5 mm
Cone base angle α	8°	22°	4°
Deviation distance or radius of blind region br	0.14 mm	1.07 mm	0.035 mm

Experiment I: The bi-cone lens used in this experiment was made of CR-39. This material is known for its low dispersion, low chromatic aberration, high transparency, and good resistance to scratch. The lens has a thickness d , which equals 1.5 mm, and a base angle α of 8°. A lens of these parameter values gives a deviation distance 0.14 mm. The Simple shapes, shown in Figure 7, have been used to test this bi-cone lens, and the results are discussed in the next section.

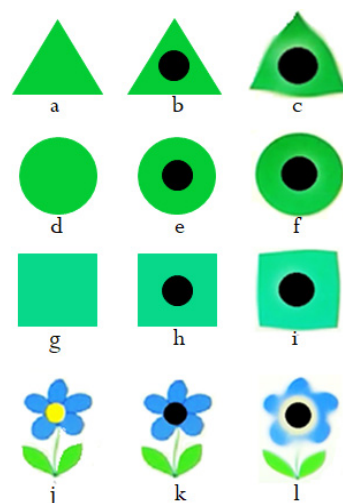


Figure 7. Demonstration of the use experiment I bi-cone lens. (a,d,g,j): original shapes, (b,e,h,k): simulation of how these shapes can be seen by a patient with central vision loss, and (c,f,i,l): images captured when using the bi-cone lens with the central regions of each shape appearing as rings of lighter colors around the black circle.

Experiment II: the waveguide or bi-cone lens used in this experiment was made of PMMA. PMMA has good resistance to environmental conditions, high clarity, good chemical resistance, high heat resistance, high hardness, and good UV blocking. It also has

a high compatibility degree with human tissue, which is why contact lenses and intraocular lenses are made of PMMA [35,36]. The bi-cone ophthalmic lens used in this experiment is of 4 mm thickness d and 22° cone base angle α . Therefore, it gives a ray deviation br of about 1.07 mm. This lens has been tested with the English text shown in Figure 8 to demonstrate the validity of the proposed lens in reading. The obtained results are presented and discussed later.

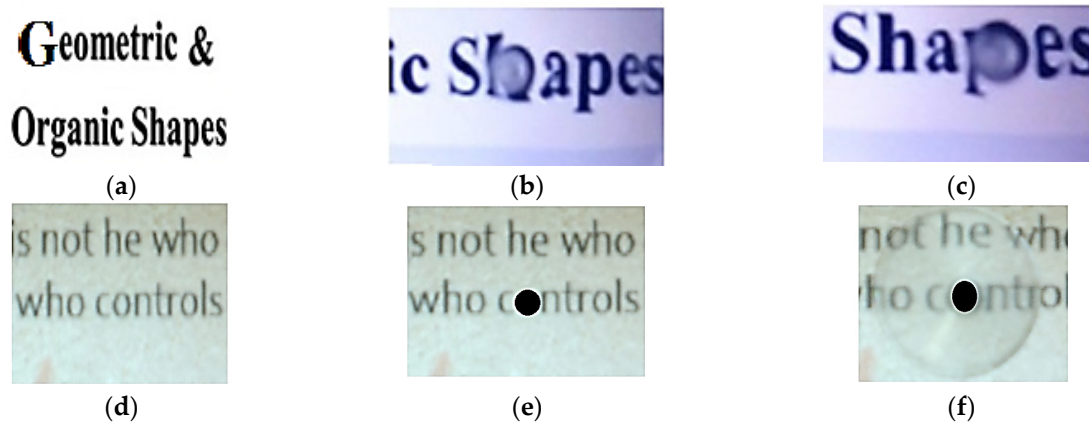


Figure 8. Effect of using the proposed bi-cone lens in reading. (a,d) The original scenes, (b,c,e,f) the obtained results.

Experiment III: the proposed bi-cone lens was made of CR-39 with 1.5 mm thickness d and a cone base angle α of 4° . With these parameter values, this lens gives a blind region radius br of about 0.035 mm. This lens has been used to visualize scenes at long distances to prove the feasibility of the proposed solution in waking and driving to avoid accidents. The obtained results are discussed in the next section of this article.

Clinical trials: As a proof of concept, the three lenses were tried by three volunteers. Those volunteers have different cases of central vision loss. The description of these cases is as follows:

- The first case is a fifty-nine-year-old woman who has a central vision loss of about 90% of her left eye. She can hardly see things like big objects during the day.
- The second case is a sixty-five-year-old man with an early AMD of less than 1 mm diameter central vision loss.
- The third case is a thirty-three-year-old man who does not have central vision loss. In each of his eyes, he has a moving translucent spot in the vitreous body which blocks most of the light going through it. This leads to a vision disorder similar to having a moving hazy region in the retina. This patient stated that he got mad when this spot aligned with the center of the eye as it feels like fog covering most of the central region of the scene.

3. Results and Discussion

Ophthalmic glasses and visual aids are case-dependent, which means the lens should be customized to suit the patient. Also, it is known that the user of new glasses or any visual aid needs some time to become accommodated with them. Because of these facts, the camera specifications, and the allowed space for experimental work, we tried to obtain some promising results with the fabricated lenses to prove the concept. Hence, with the lens described in experiment I, the most promising results were obtained with the shapes shown in Figure 7. The best results for reading-simulated trials were obtained with the lens described in experiment II. Also, the best results of walking- and driving-simulated trials were obtained with the lens described in experiment III.

Experiment I: The shapes shown in the left column of Figure 7 were used to test the validity of the bi-cone lens of experiment I. The central column of Figure 7 is a simulation

of how the patient with central vision loss or AMD can see such shapes. The bi-cone lens was placed between the shape and the camera and the distance was changed until the best results were obtained. In all pictures taken by the camera, the central region was somehow dark with no details in the center. The central details of the object appeared in a ring around the dark region, as shown in the right column of Figure 7. This is really promising, indicating that salient details can be conveyed to fall on the healthy parts of the retina in patients with central vision loss. The blackspots shown in this right column were placed intentionally to make these rings more obvious. Some deformation of the edges of shapes can be formed due to the aberration expected to be in any lens. In Figure 7c,f,i, rings of lighter green are seen as the results of using the bi-cone lens. The result is very clear in Figure 7l where the yellow detail at the center of the flower appears as a yellowish-white ring around this central region in the image. Black spots are placed on the images to make the rings more obvious.

Experiment II: The bi-cone lens described in experiment II showed the best results in reading-simulated trials investigating the validity of the proposed lens for reading. Figure 8a,d shows the original pieces of pages containing English text. The proposed lens was placed between the paper and the camera and moved until the best pictures were obtained. Note the deformation that occurred with the letters “b” and “p” in the images shown in Figure 8b,c, respectively. Instead of being blocked, these parts of the letters were conveyed from the center of the blind region to be observed, which means if used with a patient, these letters can be recognized. Figure 8e,f shows more results when trying to simulate the reading of the word “controls” while the letter “o” is assumed to fall on the blind region. The result in Figure 8e was not satisfactory, where the distance between the camera and the lens is 5 cm. Moving the camera to keep a distance of 3 cm with the lens, the ring representing the letter “o” appeared as a lighter gray ring. The black spot is placed to make the gray ring more obvious in the figure. This means that the patient must get trained to accommodate such lenses, as is usually done with new glasses. Naturally, more training is required with visual aids for such intimidating disorders.

Experiment III: The lens described in the previous section was tested with outdoor long-distance scenes for experiment III, as shown in Figures 9 and 10. A minaret observed from about 700 m distance is shown in Figure 9a. The way the patient, with a very early AMD, can see this minaret from this distance is simulated in Figure 9b. The image captured while placing the lens in front of the camera is shown in Figure 9c. It is clear that the blocked part of the minaret appears deformed while the illuminated small part (window of the minaret) gives a greenish appearance. This result is really promising for the conclusion that the lenses can be used for walking to know if there is an object or obstacle in order to avoid accidents.

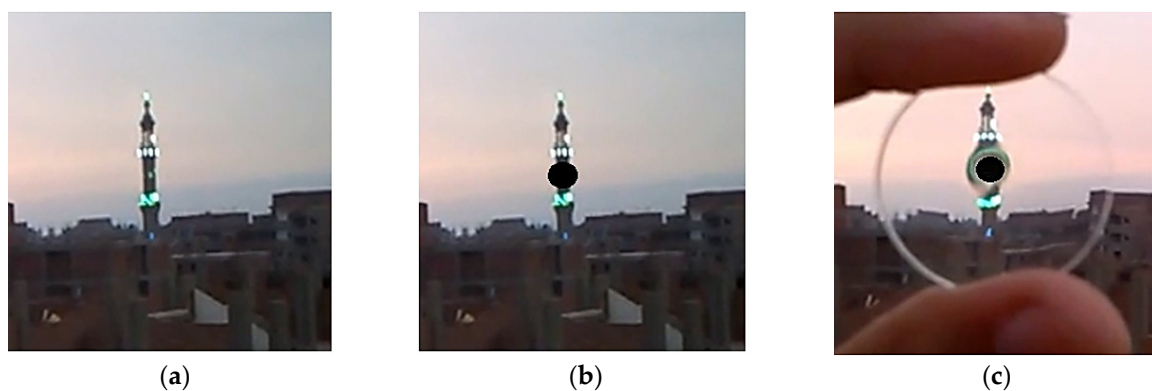


Figure 9. Testing the feasibility of using the proposed lens during walking: (a) a minaret original scene from about 700 m distance, (b) simulating how the scene can be observed by a central vision loss patient, and (c) the scene captured when placing the bi-cone lens before the camera with the hidden details of (b) appearing as a spatially-deformed region.

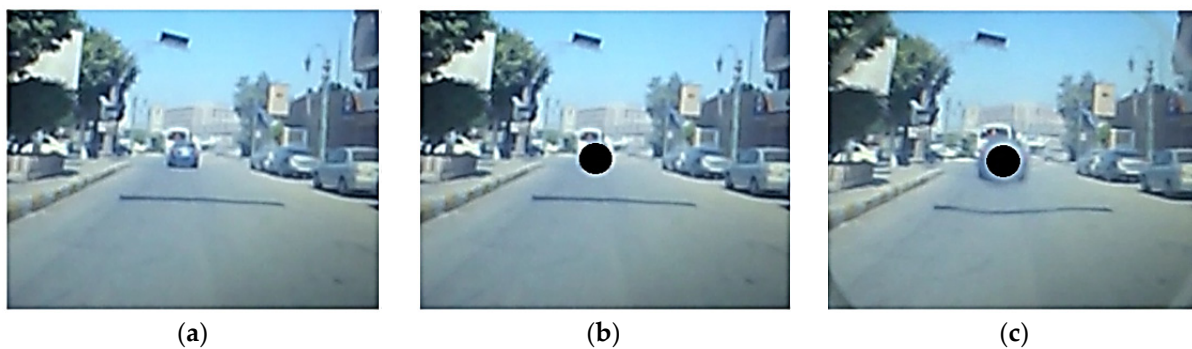


Figure 10. Testing the feasibility of using the proposed lens during driving: (a) a street original scene with a white bus and a gray sedan car. (b) Simulation of how the scene can be observed by a central vision loss patient while the car is blocked. (c) The scene captured when placing the bi-cone lens before the camera, with the hidden car in (b) appearing as a spatially-deformed region in (c).

Other measurements were taken during driving, as shown in Figure 10. The original scene is shown in Figure 10a containing a white bus and a gray sedan car behind it. The scene for an AMD patient is simulated in Figure 10b where the gray sedan car completely blocked. Placing the lens before the camera, the image in Figure 10c was obtained. Investigating Figure 10c, it is clear that the lens performed spatial transformation and conveyed the blocked details of the gray car to outside the circumference of the blind region. The car appears as a gray ring with two small dark details representing the rare tires. If a patient uses a similar lens, he/she can expect that there is a car behind the bus.

Results of clinical trials: After obtaining such promising results, the lenses were tried with the three volunteer cases described in the previous section, and the obtained results are discussed below. Recalling that the three lenses used in experiments I, II, and III apply a deviation distance or blind region radius br of 0.14, 1.07, and 0.035 mm, respectively, we can order them by their deviation ability to small deviation for experiment III, medium deviation for experiment I, and considerable deviation for experiment II.

- The first case of malfunctioning left eye tried the three lenses and the results are discussed in the following three points:
 - With the small deviation lens, she got upset and removed it quickly, which means that the lens distorted the very big details she used to recognize on the peripheries. This is expected when using a lens not suitable for the patient. It is expected that the lens conveyed a very small central region but not to the healthy parts of the retina of this patient since she has about 90% central vision loss.
 - Trying the medium deviation lens, she said that she did not feel as bad as the previous one but there was no sight improvement.
 - With the considerable deviation lens, the patient was excited as she started to recognize some more details as a color appeared on a building about 200 m away. Based on these trials, we can say that the proposed solution is promising and can be customized to meet the patient's case and needs.
- The second case of early AMD tried the three lenses and unlike the first case, he was happy with the small deviation lens, especially after a short period of time. He mentioned that he recognized the missed part and suggested having it as a contact lens. He also mentioned that by using a contact lens, he can move his eyes freely without the need to continuously move the lens to centralize it with the pupil. The response of this patient was really encouraging and gave great hope to everyone. As expected, this patient could not cope with the other two lenses as he already had a very small blind region.
- The third case of the moving hazy spot also tried the three lenses when the lesion was at the center. With the small deviation lens, he said that there was no improvement. But with the other two lenses, he was happy because he could see much better than

without the lens. But he also said that he can see better if the hazy spot is aligned at the periphery. This was expected as he can see normal scene details in the central part of the retina and peripheral parts uncovered by the hazy spot. It took a long time for this patient to have the hazy spots at the center to try the lens.

4. Conclusions

In conclusion, an optically augmented vision aid for patients with central vision loss has been provided. The feasibility of this aid has been investigated and proved through experimental work with simulation. It has also been tried with three volunteer patients with vision disorders including an early AMD, a severe central vision loss, and a moving hazy spot case. The proposed solution is entirely optical which means it is safe and just an ophthalmic glass. The optically augmented vision aid is claimed to outperform the current electronically augmented visual aid by getting rid of all of the drawbacks. Besides the fact that it is safe, it has no bulky structure, unlike the current solution which uses a display, a camera, and a video processing unit. The optical solution is user-friendly and enables the patient to recognize the missed details while seeing natural scenes. No harmful electric fields can be generated with the use of the proposed solution. Although the current solution displays the processed image in real time, it of course cannot reach the speed of light propagation as is done with optical processing. Based on the obtained results, the proposed optically augmented vision aid is foreseen to provide patients with central vision loss with necessary aid.

Author Contributions: Conceptualization, N.H.S. and H.A.; methodology, N.H.S., N.N. and Y.G.; validation, N.H.S. and Y.G.; formal analysis, Y.G.; investigation, Y.G.; resources, N.N. and Y.G.; data curation, H.A.; writing—original draft, N.N., H.A. and Y.G.; supervision, N.H.S.; project administration, N.H.S.; funding acquisition, N.H.S. All authors have read and agreed to the published version of the manuscript.

Funding: This work was supported by the Deanship of Scientific Research, Vice Presidency for Graduate Studies and Scientific Research, King Faisal University, Saudi Arabia [Grant5,863].

Institutional Review Board Statement: Not applicable.

Informed Consent Statement: Not applicable.

Data Availability Statement: Data are contained within the article.

Acknowledgments: The experimental work is acknowledged to the Biophotonics lab at the National Institute of Laser Enhanced Sciences, Cairo University.

Conflicts of Interest: The authors declare no conflict of interest.

References

1. Ackland, P.; Resnikoff, S.; Bourne, R. World blindness and visual impairment: Despite many successes, the problem is growing. *Community Eye Health* **2018**, *30*, 71–73.
2. Pascolini, D.; Mariotti, S.P. Global estimates of visual impairment: 2010. *Br. J. Ophthalmol.* **2012**, *96*, 614–618. [[CrossRef](#)]
3. Yang, L.; Yan, S.; Xie, Y. Detection of microaneurysms and hemorrhages based on improved Hessian matrix. *Int. J. Comput. Assist. Radiol. Surg.* **2021**, *16*, 883–894. [[CrossRef](#)]
4. Hinton, D.R.; Wilkinson, C.P.; Wiedemann, P. *Retina*; Elsevier Health Sciences: Amsterdam, The Netherlands, 2013; Volume 2.
5. Hildebrand, G.D.; Fielder, A.R. Anatomy and Physiology of the Retina. In *Pediatric Retina*; Springer: Berlin/Heidelberg, Germany, 2011; pp. 39–64. [[CrossRef](#)]
6. Heus, P.; Verbeek, J.H.; Tikka, C. Optical correction of refractive error for preventing and treating eye symptoms in computer users. *Cochrane Database Syst. Rev.* **2018**, *4*, CD009877. [[CrossRef](#)]
7. Kyari, F.; Abdull, M.M. The basics of good postoperative care after glaucoma surgery. *Community Eye Health* **2016**, *29*, 29–31.
8. Sahel, J.A.; Marazova, K.; Audo, I. Clinical characteristics and current therapies for inherited retinal degenerations. *Cold Spring Harb. Perspect. Med.* **2015**, *5*, a017111. [[CrossRef](#)] [[PubMed](#)]
9. Alsharafi, S.; Solouma, N.; Fathy, M.; Youssef, A.B. A New Computer-Aided Laser Photocoagulation Technique for the Treatment of Retinal Disorders. In Proceedings of the BioMed 2011, Innsbruck, Austria, 17–19 February 2011.
10. Hamdy, O.; Alsharafi, S.S.; Hassan, M.F.; Eldib, A.; Solouma, N.H. A multi-spot laser system for retinal disorders treatment: Experimental study. *Opt.-Int. J. Light Electron Opt.* **2019**, *185*, 609–613. [[CrossRef](#)]

11. Willoughby, C.E.; Ponzin, D.; Ferrari, S.; Lobo, A.; Landau, K.; Omid, Y. Anatomy and physiology of the human eye: Effects of mucopolysaccharidoses disease on structure and function—A review. *Clin. Exp. Ophthalmol.* **2010**, *38*, 2–11. [[CrossRef](#)]
12. Mahabadi, N.; Al Khalili, Y. *Neuroanatomy, Retina*; StatPearls Publishing LLC: St. Petersburg, FL, USA, 2021.
13. Mebed, R.; Ali, Y.B.M.; Solouma, N.; Eldib, A.; Amer, M.; Osman, A. Rhodopsin mutations are scarcely implicated in autosomal recessive retinitis pigmentosa: A preliminary study of Egyptian retinitis pigmentosa patients. *Egypt. J. Med. Hum. Genet.* **2015**, *16*, 355–359. [[CrossRef](#)]
14. Chawla, A.; Chawla, R.; Jaggi, S. Microvascular and macrovascular complications in diabetes mellitus: Distinct or continuum? *Indian J. Endocrinol. Metab.* **2016**, *20*, 546–553. [[CrossRef](#)] [[PubMed](#)]
15. Nian, S.; Lo, A.C.Y.; Mi, Y.; Ren, K.; Yang, D. Neurovascular unit in diabetic retinopathy: Pathophysiological roles and potential therapeutical targets. *Eye Vis.* **2021**, *8*, 15. [[CrossRef](#)]
16. Duh, E.J.; Sun, J.K.; Stitt, A.W. Diabetic retinopathy: Current understanding, mechanisms, and treatment strategies. *JCI Insight* **2017**, *2*, e93751. [[CrossRef](#)]
17. Bhutto, I.; Luty, G. Understanding age-related macular degeneration (AMD): Relationships between the photoreceptor/retinal pigment epithelium/Bruch's membrane/choriocapillaris complex. *Mol. Asp. Med.* **2012**, *33*, 295–317. [[CrossRef](#)]
18. Kivinen, N. The role of autophagy in age-related macular. *Acta Ophthalmol.* **2018**, *96*, 7–50. [[CrossRef](#)]
19. Lock, J.H.J.; Fong, K.C.S. An update on retinal laser therapy. *Clin. Exp. Opt.* **2011**, *94*, 43–51. [[CrossRef](#)]
20. Markolf, N.H. *Laser-Tissue Interactions: Fundamentals and Applications*; Springer: Berlin/Heidelberg, Germany, 2007.
21. Piotter, E.; McClements, M.E.; Maclaren, R.E. Therapy Approaches for Stargardt Disease. *Biomolecules* **2021**, *11*, 1179. [[CrossRef](#)]
22. Crane, R.; Conley, S.M.; Al-ubaidi, M.R.; Naash, M.I. Gene Therapy to the Retina and the Cochlea. *Front. Neurosci.* **2021**, *15*, 652215. [[CrossRef](#)]
23. Lu, L.J.; Liu, J.; Adelman, R.A. Novel therapeutics for Stargardt disease. *Graefe's Arch. Clin. Exp. Ophthalmol.* **2017**, *255*, 1057–1062. [[CrossRef](#)]
24. Iskander, M.; Ogunsola, T.; Ramachandran, R.; McGowan, R.; Al-Aswad, L.A. Virtual Reality and Augmented Reality in Ophthalmology: A Contemporary Prospective. *Asia-Pac. Acad. Ophthalmol.* **2021**, *10*, 244–252. [[CrossRef](#)] [[PubMed](#)]
25. Aydınođan, G.; Kavaklı, K.; Şahin, A.; Artal, P.; Ürey, H. Applications of augmented reality in ophthalmology [Invited]. *Biomed. Opt. Express* **2021**, *12*, 511–538. [[CrossRef](#)] [[PubMed](#)]
26. Venkatesan, M.; Mohan, H.; Ryan, J.R.; Schürch, C.M.; Nolan, G.P.; Frakes, D.H.; Coskun, A.F. Virtual and augmented reality for biomedical applications. *Cell Reports Med.* **2021**, *2*, 100348. [[CrossRef](#)] [[PubMed](#)]
27. Lawton, T. Improved word performance Using Individualized Compensation Filters for Observers with Losses in Central Vision. *Ophthalmology* **1989**, *96*, 115–126. [[CrossRef](#)] [[PubMed](#)]
28. Peli, E.; Goldstein, R.B.; Young, G.M.; Trempe, C.L.; Buzney, S.M. Image Enhancement For The Visually Impaired. *Investig. Ophthalmol. Vis. Sci.* **1991**, *32*, 2337–2350. [[CrossRef](#)]
29. Peli, E.; Luo, G.; Bowers, A.; Rensing, N. Applications of augmented-vision head-mounted systems in vision rehabilitation. *J. Soc. Inf. Disp.* **2007**, *15*, 1037–1045. [[CrossRef](#)] [[PubMed](#)]
30. Zhao, Y.; Szpiro, S.; Shi, L.; Azenkot, S. Designing and evaluating a customizable head-mounted vision enhancement system for people with low vision. *ACM Trans. Access. Comput.* **2019**, *12*, 15. [[CrossRef](#)]
31. Peli, E.; Luo, G.; Bowers, A.; Rensing, N. 22.4: Invited Paper: Augmented Vision Head-Mounted Systems for Vision Impairments. *SID Symp. Dig. Tech. Pap.* **2007**, *38*, 1074–1077. [[CrossRef](#)]
32. Htike, H.M.; Margrain, T.H.; Lai, Y.K.; Eslambolchilar, P. Ability of head-mounted display technology to improve mobility in people with low vision: A systematic review. *Transl. Vis. Sci. Technol.* **2020**, *9*, 26. [[CrossRef](#)] [[PubMed](#)]
33. Hwang, A.D.; Peli, E. Augmented edge enhancement on google glass for vision-impaired users. *Inf. Disp.* **2014**, *30*, 16–19. [[CrossRef](#)]
34. Gross, H.; Blechinger, F.; Ahtner, B. *Handbook of Optical Systems, Volume 4: Survey of Optical Instruments*; Wiley: Hoboken, NJ, USA, 2015.
35. Arba-Mosquera, S.; Triefenbach, N. Analysis of the cornea-to-PMMA ablation efficiency rate. *J. Mod. Opt.* **2012**, *59*, 930–941. [[CrossRef](#)]
36. Shen, J.H.; Joos, K.M.; Manns, F.; Ren, Q.; Fankhauser, F.; Denham, D.; Söderberg, P.G.; Parel, J.M. Ablation rate of PMMA and human cornea with a frequency-quintupled Nd:YAG laser (213 nm). *Lasers Surg. Med.* **1997**, *21*, 179–185. [[CrossRef](#)]

Disclaimer/Publisher's Note: The statements, opinions and data contained in all publications are solely those of the individual author(s) and contributor(s) and not of MDPI and/or the editor(s). MDPI and/or the editor(s) disclaim responsibility for any injury to people or property resulting from any ideas, methods, instructions or products referred to in the content.